

Physical Properties of Biochar

Adriana Downie, Alan Crosky and Paul Munroe

Introduction

The physical properties of biochars contribute to their function as a tool for environmental management. Their physical characteristics can be both directly and indirectly related to the way in which they affect soil systems. Soils each have their own distinct physical properties depending upon the nature of mineral and organic matter, their relative amounts and the way in which minerals and organic matter are associated (Brady and Weil, 2008). When biochar is present in the soil mixture, its contribution to the physical nature of the system may be significant, influencing depth, texture, structure, porosity and consistency through changing the bulk surface area, pore-size distribution, particle-size distribution, density and packing. Biochar's effect on soil physical properties may then have a direct impact upon plant growth because the penetration depth and availability of air and water within the root zone is determined largely by the physical make-up of soil horizons. The pres-

ence of biochar will, by affecting these physical characteristics, directly affect the soil's response to water, its aggregation, workability during soil preparation, swelling-shrinking dynamics and permeability, as well as its capacity to retain cations and its response to ambient temperature changes. In addition, indirectly, many chemical and biological aspects of soil fertility can be inferred from physical properties, such as the physical presentation of sites for chemical reactions and the provision of protective habitats for soil microbes (Brady and Weil, 2008).

This chapter focuses on the physical (structural) characteristics of freshly made biochars, relating how their qualities are influenced by both the original organic material and the processing conditions under which the biochar is made. Where possible, these physical characterizations are discussed in the context of soil systems.

Biochars: Old and new

Two approaches that one could take in examining biochars in soils include the study of biochars that have been anthropogenically or naturally incorporated within soil systems and the study of biochar made from known feed material under known conditions. Both approaches have their advantages and challenges and complement one another in developing an understanding of how the physical nature of biochars influences soil systems over time. The Black Carbon Steering Committee, for example, has developed refer-

ence materials, including wood and grass biochar produced under standardized atmospheric conditions in a pilot-scale pyrolysis oven that are intended to represent natural samples (created by forest fires) for the purpose of cross-calibration of analysis techniques (Hammes et al, 2007). As the science advances and experimental research continues, hopefully results from the two approaches will align and ancient biochar-amended soils can be more thoroughly understood to the advantage of modern agriculture.

Relevance of extended literature

There are a limited number of peer-reviewed research papers directly presenting data on the physical characterization of biochars. Some creativity, therefore, has to be applied in literature reviews, with insightful data available from papers discussing chars made for gunpowder (Gray et al, 1985) as one example. The majority of the work on pyrolysed biomass carbons (C) has been done in the interest of developing more effective activated carbons. From a physical perspective, activated carbons are black C with both high internal surface area and microporosity, and are widely used as adsorbents in separation and purification processes for gases, liquids and colloidal solids. They also often serve as catalysts and catalyst supports. Activated carbon, however, is an expensive commodity and it is unlikely that land managers will ever afford its application to soil. Activated carbons are made from char precursors, which are analogous to biochars – hence, the literature on activated carbons is often relevant to the study of biochars. The char precursors used for making activated carbon have been characterized by several research groups (Pastor-Villegas et al, 1993; Lua et al,

2004), including a range of biomass sources such as agriculture and forest residues. These precursor products are likely to be comparable to the biochars used in anthropogenically amended soils. However, some physical activation probably occurred in traditional kilns due to steam and CO₂ evolving from wet biomass feedstocks, along with some gasification due to partial oxidation with the ingress of air.

There are some characterization studies available that have endeavoured to produce synthetic chars that replicate chars produced in natural systems due to the occurrence of fire (Brown et al, 2006). However, the physical characterization of biochars has generally been performed on samples produced in reactors replicating commercial processes, which have faster heating rates and shorter residence times than traditional methods that may have been used by pre-Columbian Indians, amongst others, to produce biochar. Some characterization work has been done on traditionally made wood charcoals (see Pastor-Villegas et al, 2006); however, the reporting of these methods for biomass residues other than wood is rare. The large-

scale economic manufacture of biochar will probably be carried out in modern engineered systems due to the environmental, health and safety issues associated with traditional manufacturing methods. As a result, the study of biochars made under the faster reaction times and controlled conditions of modern processing will probably be relevant for an increasing number of biochar systems (see Chapter 9) as the science moves forward.

Another consideration is that the majority of characterization work has been performed on biochars made from biomass with high C contents and low inorganic contents (ash) in order to meet the demands of the highly specified activated carbon markets. Biochar also includes products made from high-ash (inorganic) biomass feedstocks. To date, the body of physical characterization work on these types of biochars is limited but growing.

Caution on comparing data

When reviewing the literature regarding the physical characterization of biochar, care should be taken not only because experimental conditions are highly variable, but also because they are not always reported in sufficient detail. This applies to the conditions under which the samples were prepared and the conditions under which they are analysed. For example, a commonly used physical analysis technique for determining surface areas of biochars is gas sorptometry. Adsorption experimentation is only as good as the interpretation of the results and differ-

ent methods often yield very different results. Therefore, care should be taken to only compare literature values obtained by the same method. It is known that, for microporous solids, a value of surface area does not always describe a unique property of the material but, rather, depends upon how the adsorption isotherm is determined and interpreted (Marsh, 1987). Critical review of the techniques used is beyond the scope of this chapter; however, further discussion of the issues can be found in Marsh (1987), Macias-Garcia et al (2004) and many others.

Origin of biochar structure

The physical characteristics of biochar depend not only upon the starting organic material (biomass), but also upon the carbonization or pyrolysis system by which they are made (including the pre- and post-handling of the biomass and biochar). The degree of alteration of the original structures of the biomass, through microstructural rearrangement, attrition during processing, and the formation of cracks all depend upon the processing conditions to which they are exposed.

Since biochar is a term used to refer to the high-C solid formed as the result of the

pyrolysis of organic matter, the material can have originated from a diverse range of biomass materials. The original structure of most types of materials is imprinted on the biochar product (Laine et al, 1991; Wildman and Derbyshire, 1991) and, thus, has an overwhelming influence on its final physical and structural characteristics. During pyrolysis, mass is lost (mostly in the form of volatile organics) and a disproportional amount of shrinkage or volume reduction occurs. Hence, during thermal conversion, the mineral and C skeleton formed retains the

rudimentary porosity and structure of the original material. The residual cellular structures of botanical origin that are present and identifiable in biochars from woods and coals of all ranks contribute the majority of the macroporosity present (Wildman and Derbyshire, 1991). Confirming this, microscopy analysis of physically activated carbon has illustrated the presence of aligned honeycomb-like groups of pores on the order of 10 μ m in diameter, most likely the carbonaceous skeleton from the biological capillary structure of the raw material (Laine et al, 1991). These large-sized pores serve as a feeder to lower-dimension pores (i.e. meso- and micro-pores) (Fukuyama et al, 2001; Martínez et al, 2006; Zabaniotou et al, 2008).

The chemical composition of the biomass feedstock has a direct impact upon the physical nature of the biochar produced. At temperatures above 120°C, organic materials begin to undergo some thermal decomposition, losing chemically bound moisture. Hemicelluloses are degraded at 200°C to 260°C, cellulose at 240°C to 350°C, and lignin at 280°C to 500°C (Sjöström, 1993). Therefore, the proportions of these components will influence the degree of reactivity and, hence, the degree to which the physical structure is modified during processing. The proportion of inorganic components (ash) also has implications for physical structure. Some processing conditions result in ash fusion or sintering, which can be the most dramatic change within the physical and structural composition of biochar.

Operating parameters during the pyrolysis process that influence the resultant physical properties of biochar of any given biomass feedstock include heating rate, highest treatment temperature (HTT), pressure, reaction residence time, reaction vessel (orientation, dimensions, stirring regime, catalysts, etc.), pre-treatment (drying, comminution, chemical activation, etc.), the flow rate of ancillary inputs (e.g. nitrogen, carbon dioxide, air, steam, etc.), and post-

treatment (crushing, sieving, activation, etc.).

Although all of these parameters contribute to the final biochar structure, the pyrolysis HTT is expected to be the most important of the factors studied because the fundamental physical changes (i.e. the release of volatiles, the formation of intermediate melts and the volatilization of the intermediate melts) are all temperature dependent. The temperature ranges, however, under which these stages occur vary with feedstock. Heating rates and pressures are expected to have the second greatest influence since they affect the physical mass transfer of volatiles evolving at the given temperature from the reacting particles (Antal and Grønli, 2003; Biagini and Tognotti, 2003; Lua et al, 2004; Boateng, 2007).

Lua et al (2004) evaluate the relative importance of temperature, hold time, nitrogen (N₂) flow rate and heating rate during pyrolysis by assessing the standard deviations and coefficients of variation of several physical parameters (e.g. Brunauer, Emmett and Teller equation (BET) surface area, and micropore surface area and yield). They found the pyrolysis temperature to have the most significant effect, followed by pyrolysis heating rate. The N₂ flow rate and the hold (residence) time show the least effects. It should be noted that these results are only directly relevant for their given feedstock and process conditions.

On the other hand, BET surface areas of olive kernel biochars measured by Zabaniotou et al (2008) increased with increasing mass loss (burn-off), regardless of the activation temperature. This indicates that with systems that include some higher oxidative gasification conditions, the burn-off of the fixed C has the most significant effect on increasing the surface area. Indeed, the surface area depends largely upon the C mass removed during processing, creating pores in the material (Zabaniotou et al, 2008).

An additional mechanism producing the structural complexity of biochars is the

occurrence of cracking. Biochar is typically laced with macro-cracks, which can be related to both feedstock properties and the rate at which carbonization is carried out (Byrne and Nagle, 1997). Wood biochar is generally broken and cracked due to shrinkage stresses developed because the surface of the material decomposes faster than its interior. Brown et al (2006) concluded that high-temperature (1000°C) surface area is controlled primarily by low-temperature (<450°C) cracking and high-temperature microstructural rearrangement. Through

experimentation, they found the cracks formed to be too large and too numerous to be sealed off by microstructural rearrangement at higher carbonization temperatures (Brown et al, 2006). Byrne and Nagle (1997) have developed preparation methods for wood feedstocks based on its fundamental characteristics, such as density and strength, under which C monoliths (biochars with no cracks) can be produced for advanced applications. The importance of biochar structure for macro-scale porosity is discussed later in this chapter.

Influence of molecular structure on biochar morphology

The fundamental molecular structure of biochar creates both its surface area and porosity. Carbonaceous solid materials such as coals, charcoals, cokes, etc. contain crystalline particles (crystallites) in the order of nanometres in diameter, composed of graphite-like layers arranged turbostratically (layers are not aligned) (Warren 1941; Biscoe and Warren, 1942). The biochar structure, determined by X-ray diffraction, is essentially amorphous in nature, but contains some local crystalline structure (Qadeer et al, 1994) of highly conjugated aromatic compounds. Crystalline areas can be visualized as stacks of flat aromatic (graphene) sheets cross-linked in a random manner (Bansal et al, 1988). Similar to graphite, they are good conductors in spite of their small dimensions (Carmona and Delhaes, 1978). Thus, the microcrystallites are often referred to as the conducting phase. The other non-conducting components that complete the biochar C matrix are the aromatic-aliphatic organic compounds of complex structure (including residual volatiles), and the mineral compounds (inorganic ash) (Emmerich et al, 1987). This is complemented with the voids, formed as pores (macro-, meso- and micro-pores), cracks and morphologies of cellular

biomass origin.

Pyrolysis processing of biomass enlarges the crystallites and makes them more ordered. This effect increases with HTT. Lua et al (2004) demonstrated, for example, that increasing the pyrolysis temperature from 250°C to 500°C increases the BET surface area due to the increasing evolution of volatiles from pistachio-nut shells, resulting in enhanced pore development in biochars. For turbostratic arrangements, the successive layer planes are disposed approximately parallel and equidistant, but rotated more or less randomly with respect to each other (see inset B, Figure 2.1) (Emmerich et al, 1987). The spacing between the planes of turbostratic regions of biochar is larger than that observed in graphite (Emmerich et al, 1987; Laine and Yunes, 1992). In spite of the two-dimensional long-range order in the directions of the graphite-like layers, materials with turbostratic structure are called non-graphitic C because there is no measurable crystallographic order in the third direction (insets B and C, Figure 2.1) (Emmerich and Luengo, 1996). Rosalind Franklin first demonstrated that some varieties of non-graphitic C are converted to graphitic C during pyrolysis, presenting crys-

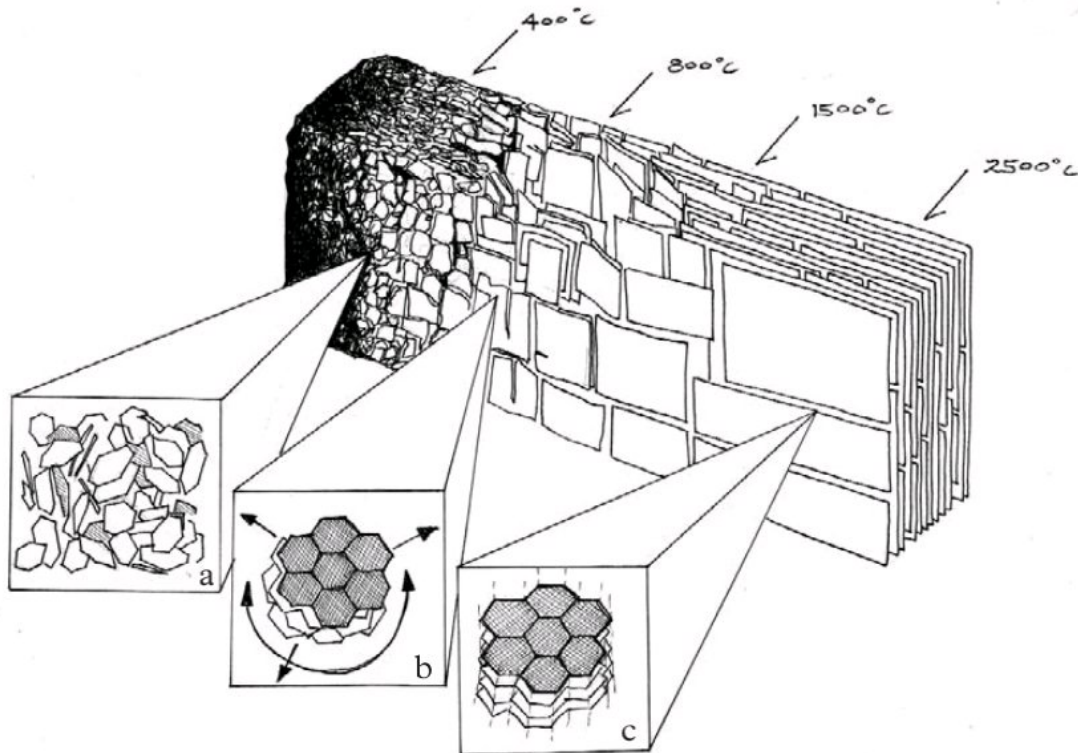


Figure 2.1 *Ideal biochar structure development with highest treatment temperature (HTT): (a) increased proportion of aromatic C, highly disordered in amorphous mass; (b) growing sheets of conjugated aromatic carbon, turbostratically arranged; (c) structure becomes graphitic with order in the third dimension*

Source: chapter authors

tallographic order in the third direction (Franklin, 1951). The pyrolysis of all biomass C will finally yield graphite when heated to 3500°C; however, some feedstocks graphitize at HTTs of less than 2000°C (Setton et al, 2002).

The surface of non-graphitized C, such as wood biochars, consists of both the faces and edges of ordered sheets (Boehm, 1994, 2002). The turbostratic linkage of these crystallites leaves random interstices (pores of various sizes). A further possible cause of micropores is from voids (holes) within hexagonal planes (Bourke et al, 2007). Heteroatoms, in particular oxygen (O), are predominantly located on the edges of ordered sheets as components of various functional groups (Boehm, 1994, 2002). The interplanar distance of graphite (0.335nm) is

probably not achieved under typical pyrolysis conditions (<1000°C) due to the formation of O functional groups at the sheet edges, which through steric or electronic effects prevent the close packing of the sheets (Laine and Yunes, 1992).

Pores, of whatever origin, may become filled with tars (condensed volatiles) and other amorphous decomposition products, which may partially block the microporosity created (Bansal et al, 1988). The tars created from thermal biomass C decomposition impede the continuity of pores at low temperatures and these pores become increasingly accessible as the temperatures increase and tar components are volatilized (Pulido-Novicio et al, 2001). Mineral matter may also become occluded in the pores or exposed at the surface of the biochar particles.

Loss of structural complexity during pyrolysis

Under certain processing conditions, many research groups have reported drastic loss of structural complexity in biochar products, which is often explained by plastic deformation, melt, fusion or sintering. High heating rates, increased pressure, high HTT, high ash contents (or low ash melting points) and long retention times (in combination with high temperatures) have all been held accountable for the loss of surface area and porosity in biochar products. Of the numerous examples in the literature some typical results have been selected to demonstrate each pathway.

Rodríguez-Mirasol et al (1993) investigated the carbonization of eucalyptus kraft lignin at different temperatures and characterized the structure of the microporous biochar product. They found that partial fusion and swelling in the carbonization stage was related to the ash content (inorganic matter) in the starting material (Rodríguez-Mirasol et al, 1993). Therefore, they developed a new pre-treatment method to remove the inorganic matter by washing with diluted acidic solutions prior to carbonization in order to prevent this loss of structural complexity. High ash content is often a significant contributing factor to loss of structure. However, even in very low ash materials, such as the hazelnut shell (Aygun et al, 2003), some thermoplastic properties can be exhibited.

The lack of structure in biochars made at high heating rates has been explained by the melting of the cell structure and by plastic transformations (Biagini and Tognotti, 2003; Boateng, 2007). Cetin et al (2004) reported that at low heating rates ($20^{\circ}\text{C sec}^{-1}$), the natural porosity of pine sawdust allows a volatile release with the occurrence of no major morphological changes. However, at high heating rates ($500^{\circ}\text{C sec}^{-1}$), the cell structure is destroyed by devolatilization (Cetin et al, 2004). Biagini and Tognotti

(2003) recorded the same phenomenon in their experimentation and noted the re-solidification of the solid structure and formation of more compact biochar particles (Biagini et al, 2003). They also stated that melting and swelling are more pronounced for biomass species that contain higher levels of volatile matter.

High HTT, coinciding with the ash melting points of the various biomass feedstocks, also causes decreases in structural complexity. For a pistachio-nut feedstock, Lua et al (2004) found that increasing HTT from 500°C to 800°C progressively decreased the BET surface area. They attributed this to the decomposition and softening of some volatile fractions to form an intermediate melt in the biochar structure (Lua et al, 2004). Brown et al (2006) reported similar findings with biochars made from pine. At heating rates of $30^{\circ}\text{C hr}^{-1}$ and $200^{\circ}\text{C hr}^{-1}$, surface areas were found to be markedly lower at a HTT of 1000°C compared with those observed at lower final temperatures (Brown et al, 2006).

Increasing the reaction retention time has also been demonstrated to cause deformation in the physical structure; however, this may be the result of heat transfer rates being too slow for the solid to reach a high HTT. Guo and Lua (1998) found that at 900°C , the high surface area of oil palm stone biochar deteriorated with increasing reaction retention time. They attributed this to both the sintering effect, followed by a shrinkage of the biochar, and realignment of the biochar structure, which resulted in reduced pores. With their reactor configuration, they found that maximum surface areas were obtained when oil palm stones were pyrolysed at 800°C with a retention time of three hours (Guo and Lua, 1998).

Work by Lewis (2000) with redwood has shown, however, that the pores do not collapse as suggested by Guo and Lua (1998). Lewis

(2000) provides evidence against such collapse by showing that the pores can be reopened by a CO₂ activation process in a manner that allows N₂-accessible surface area to increase from 2m² g⁻¹ to 540m² g⁻¹. This suggests that the pores are still present (not collapsed) and that they are only closed off at higher temperatures (Lewis, 2000).

The fusion of multiple particles, which did not occur under atmospheric conditions,

has also been reported at pressures of 10bar to 20bar (Cetin et al, 2004). Cetin et al (2004) found that at these pressures, eucalyptus sawdust particles melt and fuse, losing their own distinctions. Similar results were obtained at atmospheric pressures for the fast heating rate of ~500°C min⁻¹. A number of particles fused together can form a hollow and smooth-surfaced particle (Cetin et al, 2004).

Industrial processes for altering the physical structure of biochar

Processes for increasing surface areas and porosity have been frequently investigated, driven by the many commercial applications of activated carbons that require large sorptive capacities. Although, as already highlighted, process conditions such as HTT, heating rate, etc. influence biochar's physical structure, commercially viable internal surface areas are almost always generated in high C-containing biochar precursors through physical or chemical activation.

Physical activation, which is carried out most frequently in industry, is obtained when the initial pyrolysis reactions, occurring in an inert atmosphere at moderate temperatures (400°C to 800°C), are complemented by a second stage in which the resulting biochars are subjected to a partial gasification at a higher temperature (usually >900°C) with oxidizing gases such as steam, CO₂, air or a mixture of these. This produces final products with well-developed and accessible internal pores (Bansal et al, 1988).

The activation of biochar with CO₂ involves a C-CO₂ reaction (Rodríguez-Reinoso and Molina-Sabio, 1992). This leads to the removal of C atoms or burn-off, in this way contributing to the development of a porous structure. According to Rodríguez-Reinoso et al (1992), CO₂ can open closed

pores as well as widen existing pores by the activation, increasing the accessibility of the small pores to the molecules of an adsorbate. Both the surface area and the nature of porosity are significantly affected by the conditions of CO₂ activation, the extent of which depends upon the nature of the precursors (Zhang et al, 2004). Steam is suggested to play a double role: it promotes both the release of volatiles with partial devolatilization and enhances crystalline C formation (Alaya et al, 2000).

The physical and adsorptive properties of biochars depend upon activation time and quantity of steam used for activation. BET surface areas of activated olive kernel carbons were found to be increasing with activation time and temperature from a minimum value of 1339m² g⁻¹ at one hour and 800°C to a maximum of 3049m² g⁻¹ at four hours and 900°C (Stavropoulos, 2005). Zhang et al (2004) confirmed these trends for biochars made from oak, maize hulls and maize stover residues. They found BET surface areas of all activated carbons obtained at 700°C were lower than those obtained at 800°C (Zhang et al, 2004). With physical activation for one to two hours, surface areas were increased with activation time (Zhang et al, 2004). This expansion in surface area with increased activation time can also be explained by the

increasing burn-off (mass loss) (Zabaniotou et al, 2008).

Chemical activation entails the addition of materials such as zinc salts or phosphoric acid to the C precursors (H_3PO_4 , ZnCl_2 and alkali metal hydroxides). KOH (and NaOH) has been used for preparing activated carbons with unusually high surface areas called 'super active' carbons by some authors (Rouquerol et al, 1999). During activation, potassium (K) is intercalated and forces apart the lamellae of the crystallites that form the C structure. After washing the samples, K is eliminated, leaving free interlayer space that contributes to the porosity of the product (Marsh et al, 1984). Precursor material properties such as microcrystalline structure, reactivity and pore accessibility are shown to affect the results of these treatments. The most suitable raw materials for KOH activation are those having small-sized crystallites, medium reactivity and high accessibility to the internal pore structure (Stavropoulos, 2005).

Chemical activation offers several advantages since it is carried out in a single step, combining carbonization and activation, is performed at lower temperatures and, therefore, results in greater development of porous structure. Chemical activation methods are not, however, as common, possibly due to the possibility of generating secondary environmental pollution during disposal (Zhang et al, 2004).

Reactor type has also been demonstrated to have an influence on the physical surface and porosity of chars. Gonzalez et al (1997) conducted their investigation of CO_2 activation with both vertical and horizontal furnaces and concluded that a horizontal furnace is advantageous for micropore development.

Biochars resulting from fast pyrolysis reactors (high heating rates) have different physical properties from those made under

slow pyrolysis conditions. The surface areas of switchgrass biochars made under fast pyrolysis conditions were found to be low, typically between $7.7\text{m}^2\text{ g}^{-1}$ and $7.9\text{m}^2\text{ g}^{-1}$ (Boateng, 2007). Further examples that are typical for fast pyrolysis, because of the high heating rates of the rather small particles (less than 1mm), were produced by a fluidized sand-bed reactor operating at approximately 500°C , with inert N_2 as the fluidizing agent (Zhang et al, 2004). Oak, maize hull and maize stover biochars exhibited low surface areas of $92\text{m}^2\text{ g}^{-1}$, $48\text{m}^2\text{ g}^{-1}$, and $38\text{m}^2\text{ g}^{-1}$, and total pore volumes of $0.1458\text{cm}^3\text{ g}^{-1}$, $0.0581\text{cm}^3\text{ g}^{-1}$ and $0.0538\text{cm}^3\text{ g}^{-1}$, respectively (Zhang et al, 2004).

Gas pressure during the pyrolysis reactions also has an influence on the structure of the biochar products. For example, biochar particles that were generated at 5bar pyrolysis pressure at a heating rate of $500^\circ\text{C sec}^{-1}$ to 950°C were shown to have larger cavities with thinner cell walls than biochars that were generated at atmospheric pressure. This effect was increased at 20bar (Cetin et al, 2004).

The pyrolysis system, particularly the activation method, has an influence on the physical nature of biochars. The degree of influence that it has, however, depends upon the feedstock used, with different feedstocks producing different results. For example, Pastor-Villegas et al (2006) found that the influence of the carbonization reaction method on the non-micropore structure is not significant when the raw material is eucalyptus wood, while there are considerable differences when the raw material is holm-oak wood (Pastor-Villegas et al, 2006). When studying biochars, it is essential to note the feedstock, preparation conditions and analysis methods used to ensure that meaningful conclusions are drawn which can be compared with that of other studies.

Soil surface areas and biochar

Surface area is a very important soil characteristic as it influences all of the essential functions for fertility, including water, air, nutrient cycling and microbial activity. The limited capacity of sandy soil to store water and plant nutrients is partly related to the relatively small surface area of its soil particles (Troeh and Thompson, 2005). Coarse sands have a very low specific surface of about $0.01\text{m}^2\text{g}^{-1}$, and fine sands about $0.1\text{m}^2\text{g}^{-1}$ (Troeh and Thompson, 2005). Clays have a comparatively large specific surface, ranging from $5\text{m}^2\text{g}^{-1}$ for kaolinite to about $750\text{m}^2\text{g}^{-1}$ for Na-exchanged montmorillonite. Soils containing a large fraction of clay may have high total water-holding capacities but inadequate aeration (Troeh and Thompson, 2005). High organic matter contents have been demonstrated to overcome the problem of too much water held in a clay soil, and also increase the water contents in a sandy soil (Troeh and Thompson, 2005). Indications exist that biochar will similarly change the

physical nature of soil, having much of the same benefit of other organic amendments in this regard (Chan et al, 2007). Biochar specific surfaces, being generally higher than sand and comparable to or higher than clay, will therefore cause a net increase in the total soil-specific surface when added as an amendment.

The influence of biochar on microbial populations in soils is presented in Chapter 6. However, it should be noted here that soil microbial biomass commonly increases with increasing clay content under both field and laboratory conditions (Amato and Ladd, 1992; Juma, 1993; Müller and Höper, 2004), and this response is generally attributed to the increased surface area (Juma, 1993). The higher surface areas of finer-textured soils can result in increased total water content and improved physical protection from grazers. Biochar has been experimentally linked to improved soil structure or soil aeration in fine-textured soils (Kolb, 2007).

Biochar nano-porosity

The pore-size distribution of activated carbons has long been recognized as an important factor for industrial application. It is logical that this physical feature of biochars will also be of importance to their behaviour in soil processes. The relationship between total surface area and pore-size distribution is logical. As shown in Figure 2.1, as the HTT increases more structured regular spacing between the planes results. Interplanar distances also decrease with the increased ordering and organization of molecules, all of which result in larger surface areas per volume.

Micropores (known to material scientists as all pores $<2\text{nm}$ in diameter) contribute

most to the surface area of biochars and are responsible for the high adsorptive capacities for molecules of small dimensions such as gases and common solvents (Rouquerol et al, 1999). It should be noted that soil scientists refer to all pores $<200\text{nm}$ in diameter as micro-pores; however, for the purpose of this chapter, the total pore volume of the biochar will be divided into micropores (pores of internal diameter less than 2nm), mesopores (pores of internal width between 2nm and 50nm) and macropores (pores of internal width greater than 50nm) (Rouquerol et al, 1999), as this provides a level of differentiation required to discuss molecular and structural effects. However, the importance

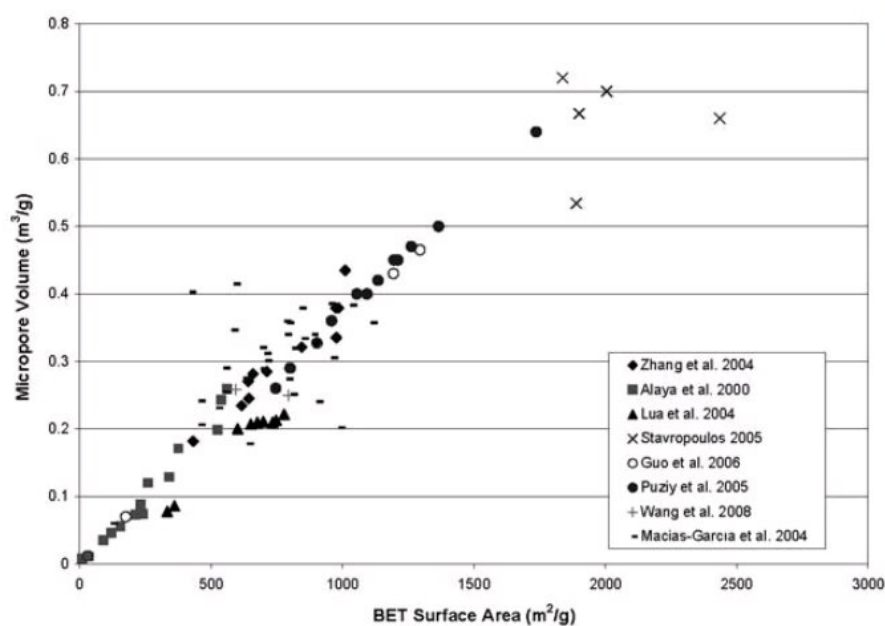


Figure 2.2 Relationship between biochar surface area and micropore volume

Source: chapter authors

and range of macroporosity in the context of biochar in soil systems cannot be overemphasized, and will be discussed in detail in a later section.

Figure 2.2 compiles some of the data available in the literature to demonstrate the relationship between micropore volume and total surface area of biochars. This provides evidence that pore sizes distributed in the micropore range make the greatest contribution to total surface area. The development of microporosity with higher temperatures and longer retention times has been demonstrated by several research groups (see plotted examples in Figure 2.3). Elevated temperatures provide the activation energies and longer retentions allow the time for the reactions to reach completion, leading to greater degrees of order in the structures. For example, the ratios of micropore volume to total pore volume of CO_2 -activated carbons produced from maize hulls generated at 700°C were lower than those of activated carbons prepared at 800°C (Zhang et al, 2004).

The analysis of gas adsorption isotherms is the typical methodology used for assessing surface areas of C materials. The range of

adsorbents, degassing regimes, temperatures, pressures and algorithms used makes comparison of literature values challenging. However, some general trends can be observed through compiling literature values (see Figure 2.3).

The surface area of biochars generally increases with increasing HTT until it reaches the temperature at which deformation occurs, resulting in subsequent decreases in surface area. A typical example is provided by Brown et al (2006), who produced biochar from pine in a laboratory oven purged with N_2 at a range of final temperatures varying from 450°C to 1000°C , and heating rates varying from 30°C hr^{-1} to $1000^\circ\text{C hr}^{-1}$. Brown et al found that independent of heating rate, maximum surface area, as measured by BET (N_2), was realized at a final temperature of 750°C . At the lowest HTT (i.e. 450°C), all of the surface areas were found to be less than $10\text{m}^2\text{ g}^{-1}$, while those produced at intermediate temperatures of 600°C to 750°C had a surface area of approximately $400\text{m}^2\text{ g}^{-1}$ (Brown et al, 2006).

Under some conditions, a high temperature causes micropores to widen because it

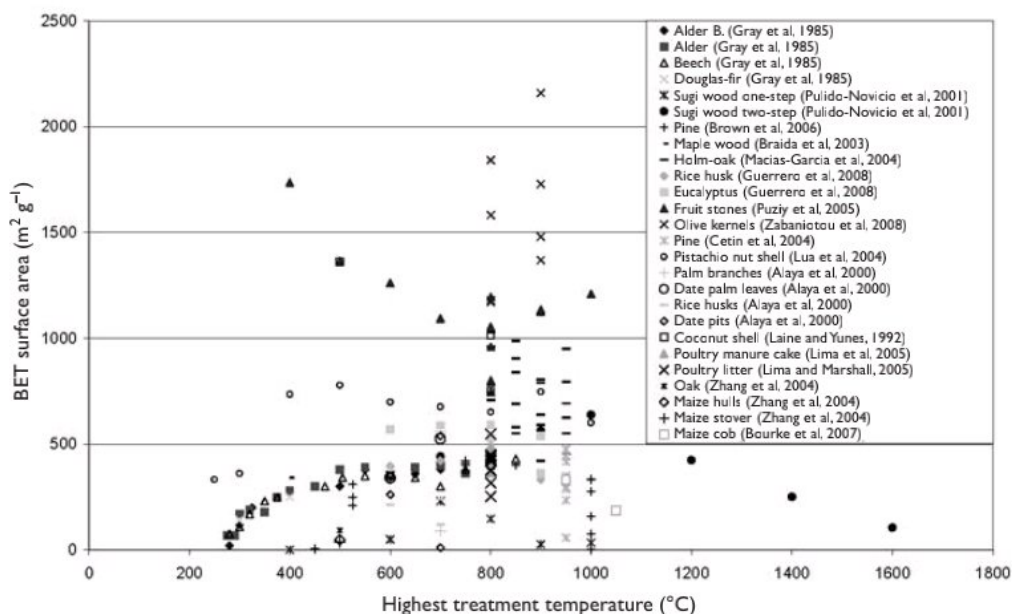


Figure 2.3 Biochar surface area plotted against highest treatment temperature (HTT)

Note: different methods of treatment and surface area analysis were used in each study.

Source: chapter authors

destroys the walls between adjacent pores, resulting in the enlargement of pores (Zhang et al, 2004). This leads to a decrease in the fraction of volume found in the micropore range and an increase in the total pore volume. In samples of maize hulls and maize stover, Zhang et al (2004) found microporosity to be appreciably greater after one hour of physical activation than after two hours. They proposed that the rate of pore formation exceeded that of destruction due to pore enlargement and collapse at the earlier stage and vice versa at the later stage (Zhang et al, 2004).

Heating rates also determine the extent of micropore formation. One example was

provided by Cetin et al (2004), who found that biochars generated at atmospheric pressure under low heating rates mainly consisted of micropores, whereas those prepared at high heating rates were largely comprised of macropores as a result of melting (Cetin et al, 2004).

Mesopores are also present in biochar materials. These pores are of importance to many liquid–solid adsorption processes. For example, pistachio-nut shells have a mixture of micropores and mesopores, with micropores dominating, indicating that these activated carbons can be used for both gas and liquid adsorption applications (Lua et al, 2004).

Biochar macroporosity

In the past, when biochars and activated carbons were assessed mainly for their role as adsorbents, macropores (>50nm diameter)

were considered to be only important as feeder pores for the transport of adsorbate molecules to the meso- and micro-pores

Table 2.1 *Surface areas and volumes of different sizes of biochar pores*

	Surface area ($m^2 g^{-1}$)	Volume ($cm^3 g^{-1}$)
Micropores	750–1360	0.2–0.5
Macropores	51–138	0.6–1.0

Source: Laine et al (1991)

(Wildman and Derbyshire, 1991). However, macro-pores are very relevant to vital soil functions such as aeration and hydrology (Troeh and Thompson, 2005). Macropores are also relevant to the movement of roots through soil and as habitats for a vast variety of soil microbes. Although micropore surface areas are significantly larger than macropore surface areas in biochars, macropore volumes can be larger than micropore volumes (see Table 2.1). It is possible that these broader volumes could result in greater functionality in soils than narrow surface areas.

As anticipated from the regular size and arrangement of plant cells in most biomass from which biochars are derived, the macropore size distribution is composed of discrete groups of pores sizes rather than a continuum (Wildman and Thompson, 1991). The obvious macroporous structure of a wood biochar imaged using a scanning electron microscope (SEM) can be seen in Figure 2.4.

To put this in perspective with typical soil particles, these discrete groups of pore diameters observed in this sample of $\sim 5\mu m$ to $10\mu m$, and $\sim 100\mu m$ compare to very fine sand or silt particle sizes, and fine sand particle sizes, respectively.

Another consideration is the type of microbial communities that utilize soil pores as a preferred habitat (see Chapter 6). Microbial cells typically range in size from $0.5\mu m$ to $5\mu m$, and consist predominantly of bacteria, fungi, actinomycetes and lichens (Lal, 2006). Algae are $2\mu m$ to $20\mu m$ (Lal, 2006). The macropores present in biochars pictured in Figure 2.4 may therefore provide suitable dimensions for clusters of microorganisms to inhabit. Chapter 6 provides more detail on microbial communities and biochar.

On the scale of soil systems, the macroporosity seen in the SEM image of a poultry litter char (see Figure 2.5), with cavities up to $500\mu m$ in the agglomerated particle, is very relevant. However, very few investigations at this scale are presented in the literature. Soil structure is defined in terms of peds, which are arrangements of primary soil particles, and soil porosity is often defined as the openness between these peds (Troeh and Thompson, 2005). The interaction and stacking of heterogenous agglomerated biochar particles and peds in the soil will have a direct impact upon the bulk soil structure.

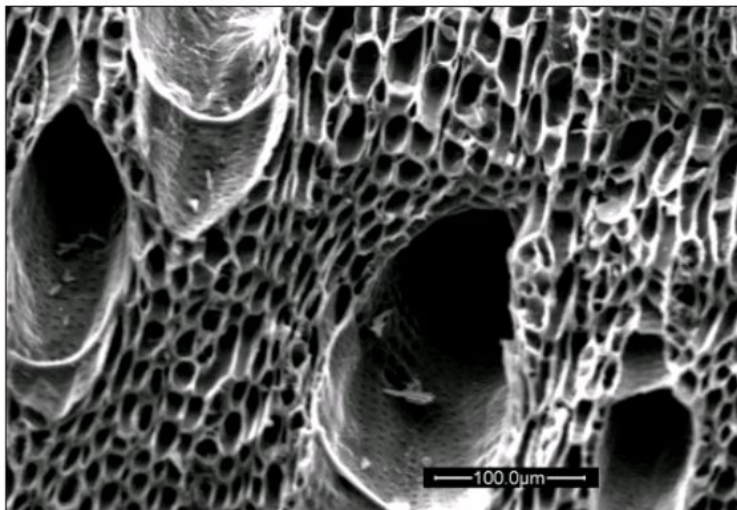


Figure 2.4 *Scanning electron microscope (SEM) image showing macroporosity of a wood-derived biochar produced by 'slow' pyrolysis: The biochar samples were chromium coated and imaged with a beam energy of 20kV on a FEI Quanta 200 environmental scanning electron microscope (ESEM)*

Source: chapter authors

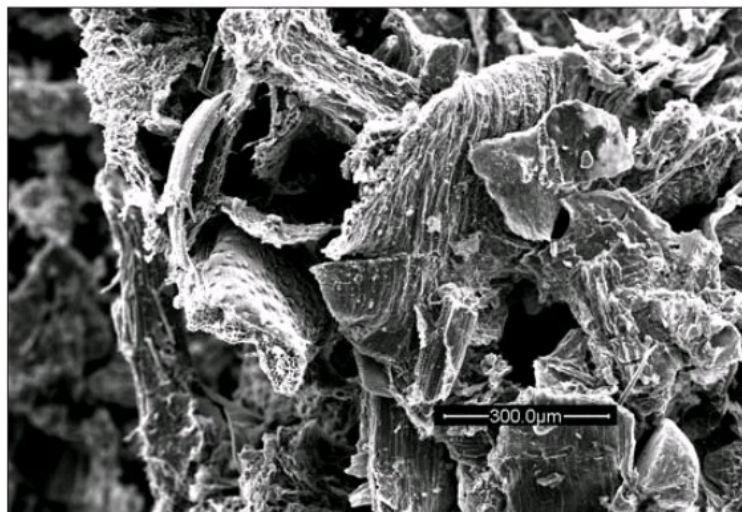


Figure 2.5 SEM image showing macroporosity in biochar produced from poultry manure using slow pyrolysis

Source: chapter authors

Particle-size distribution

The particle sizes of the biochar resulting from the pyrolysis of organic material are highly dependent upon the nature of the original material. Due to both shrinkage and attrition during pyrolysis, particle sizes of the organic matter feedstock are likely to be greater than the resultant biochar. In some cases, particles may agglomerate; therefore, increased particle sizes are also found (Cetin et al, 2004). Depending upon the mechanical intensity of the pyrolysis technology employed, a degree of attrition of the biomass particles will occur during processing. This is especially true in the post-handling of the material as the biochar is significantly more friable than the original biomass.

Evidence for the dependency of particle-size distribution of the biochar upon the organic matter feedstock is presented in Figure 2.6. Biochar derived from sawdust and wood chips was prepared with different pre-treatments, producing contrasting particle sizes. The pyrolysis processing, through the BEST Energies continuous slow ($5^{\circ}\text{C min}^{-1}$ to $10^{\circ}\text{C min}^{-1}$ heating rate) pyrolysis pilot plant, resulted in an increasing proportion of particles in the smaller size distributions for both of the feedstocks, as measured by dry sieving. It can also be seen

that as the pyrolysis HTT increased (450°C to 500°C to 700°C), the particle sizes tended to decrease. This may be explained by the decreasing tensile strength of the material as it is more completely reacted, resulting in less resistance to attrition during processing.

Depending upon the technology employed, biomass feedstock is prepared in different ways. The faster the heating rate required, the smaller the feedstock particles need to be to facilitate the heat and mass transfer of the pyrolysis reactions. Fast pyrolysis feedstocks, for example, are pre-processed to a fine dust or powder; therefore, the resultant biochar is very fine. Continuous slow pyrolysis technologies, which employ slower heating rates ($\sim 5^{\circ}\text{C min}^{-1}$ to $30^{\circ}\text{C min}^{-1}$), can accommodate larger particles up to several centimetres in dimension. Traditional batch processes can allow weeks for the heat and mass transfer of the process to occur (see Chapter 8) and, hence, receive whole branches and logs.

The investigation by Cetin et al (2004), for example, on the first-step pyrolysis of a two-stage gasification process used biomass fuel particles with sizes between $50\mu\text{m}$ and $2000\mu\text{m}$ depending upon the reactor type and techniques used. This small size is

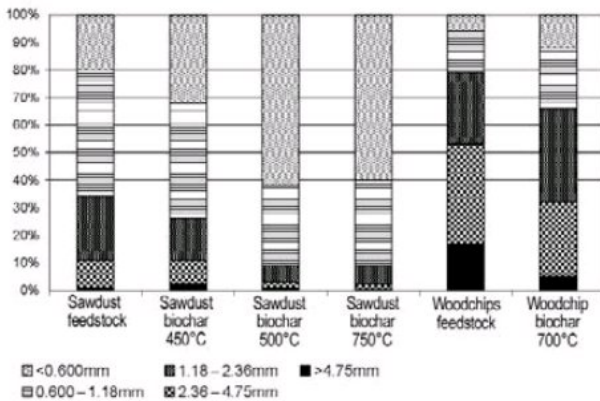


Figure 2.6 Influence of biomass pre-treatment and HTT on the particle size distribution of different biochars

Source: chapter authors

required to achieve the high heating rates, ranging from $500^{\circ}\text{C sec}^{-1}$ to extremely high heating rates of ($\approx 1 \times 10^{5^{\circ}\text{C sec}^{-1}$) and short residence times (Cetin et al, 2004).

If larger particles are used, it is possible that the reactions will be limited by the heat transfer into the particles and the mass transfer of volatiles out of the biochar. For

example, in a study of the pyrolysis of oil palm stones, it was found that the biochar yields were affected by both the particle size of the stones and the maximum pyrolysis temperature (Shamsuddin and Williams, 1992). Longer retention times would perhaps have overcome the influence of the larger particle sizes.

An increase in linear shrinkage of the particles being pyrolysed can be seen to take place in conjunction with the loss of volatile matter (Emmerich and Luengo, 1996; Freitas et al, 1997). For example, as pyrolysis temperatures increase from 200°C to 1000°C , the linear shrinkage of particles was demonstrated to increase from 0 to 20 per cent for peat biochars (Freitas et al, 1997).

Cetin et al (2004) demonstrated that increasing the pyrolysis pressure (from atmospheric to 5, 10 and 20bars) leads to the formation of larger biochar particles. They accounted for this as swelling, as well as the formation of particle clusters, as a result of melting and subsequent fusion of particles (Cetin et al, 2004).

Biochar density

Two types of density of biochars can be studied: the solid density and the bulk or apparent density. Solid density is the density on a molecular level, related to the degree of packing of the C structure. Bulk density is that of the material consisting of multiple particles and includes the macroporosity within each particle and the inter-particle voids. Often, an increase in solid density is accompanied by a decrease in apparent densities as porosity develops during pyrolysis. The relationship between the two types of densities was demonstrated by Guo and Lua (1998), who reported that apparent densities increased with the development of porosities from 8.3 to 24 per cent at pyrolysis temperatures up to 800°C (Guo and Lua, 1998). However, when the

temperature increased to 900°C , the apparent density of the biochar increased and the porosity decreased due to sintering. This inverse relationship between solid and apparent density was also demonstrated by Pastor-Villegas et al (2006) for eucalyptus biochar manufactured in a continuous furnace having both the lowest values of apparent density (measured as both bulk and mercury displacement) and the highest solid density value (measured by helium displacement).

The loss of volatile and condensable compounds from the unorganized phase of the biochars and the concomitant relative increase in the organized phase formed by graphite-like crystallites leads to the increase in solid density (or true density) of the

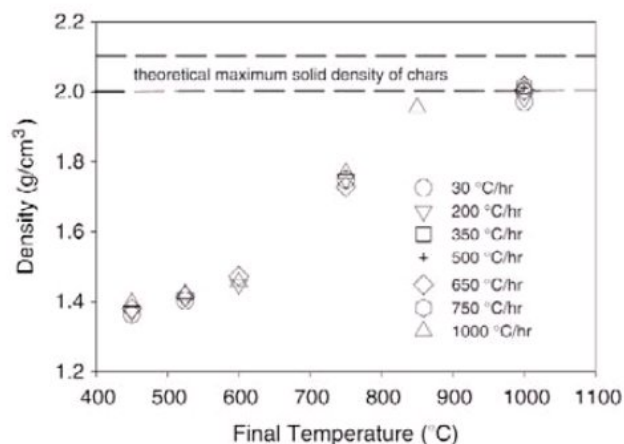


Figure 2.7 Helium-based solid densities of biochars with HTT

Source: Brown et al (2006)

biochars compared with their feedstocks (Emmerich et al, 1987). The maximum density of C in biochars has been reported to lie between 2.0 g cm^{-3} and 2.1 g cm^{-3} based on X-ray measurements (Emmett, 1948). Such values are only slightly below the density of solid graphite of 2.25 g cm^{-3} . Most solid densities of biochar, however, are significantly lower than that of graphite because of residual porosity and their turbostratic structure (Oberlin, 2002), with typical values

around 1.5 g cm^{-3} to 1.7 g cm^{-3} (Jankowska et al, 1991; Oberlin, 2002). Lower values such as that of a pine wood biochar collected from a natural fire site at 1.47 g cm^{-3} (Brown et al, 2006) are also common. Biochars activated to produce microporosity for the adsorption of gases are denser than for those optimized to produce meso- and macro-porosity for the purification of liquids (Pan and van Staden, 1998).

The density of the biochars depends upon the nature of the starting material and the pyrolysis process (Pandolfo et al, 1994). Solid density of biochar increases with increasing process temperature and longer heating residence times, in accordance with the conversion of low-density disordered C to higher-density turbostratic C (Byrne, 1996; Kercher and Nagle, 2002). Lower amounts of volatiles, which have lower molecular weights than fixed C, and lower ash contents result in higher solid density in biochars (Jankowska et al, 1991). However, Brown et al (2006) showed that density is independent of heating rate, and found a simple and direct dependency of density upon final pyrolysis temperature (see Figure 2.7). Thus, they deduced that the He-based solid density may

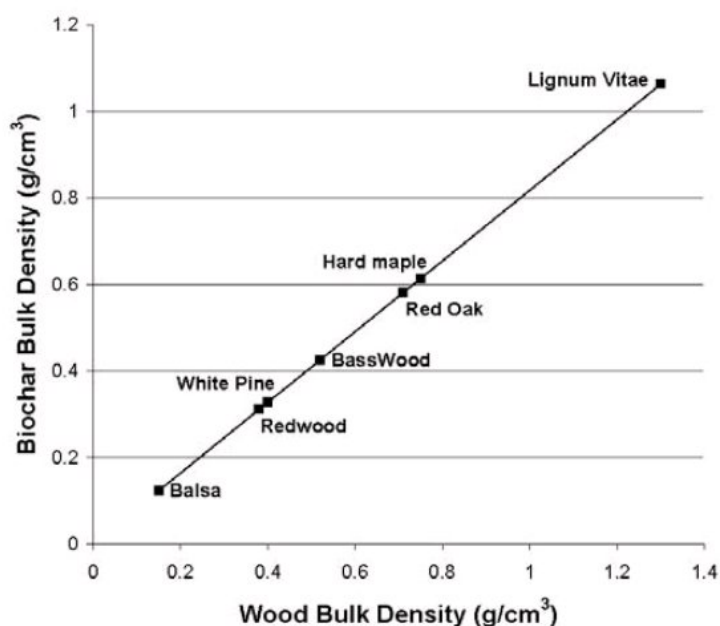


Figure 2.8 Bulk density of wood biochar, plotted against that of its feedstock

Note: Biochar bulk density = $0.8176 \times$ wood bulk density. Values are for carbonization in a nitrogen atmosphere at 15°C hr^{-1} to 900°C .

Source: Byrne and Nagle (1997)

serve as an approximate indicator of the highest temperature experienced by any wood biochar, regardless of the exact thermal history (Brown et al, 2006). This concept may provide a useful tool for characterizing charring conditions in order to understand the production of biochars in archaeological soil such as Terra Preta and possibly provide information about their creation.

Bulk density is also an important physical feature of biochars. Pastor-Villegas et al (2006) found that the bulk densities of biochars made from different types of woods processed in different types of traditional kilns ranged from 0.30 g cm^{-3} to 0.43 g cm^{-3} .

Bulk density values given in the literature for activated carbons used for gas adsorption range from 0.40 g cm^{-3} to 0.50 g cm^{-3} , while for activated carbons used for decolourization, the range is 0.25 g cm^{-3} to 0.75 g cm^{-3} (Rodríguez-Reinoso, 1997). Byrne and Nagle (1997) established a linear relationship between the bulk densities of wood and biochar made from the same material, which spans a range of species. They found that for wood pyrolysed at a heating rate of 15°C hr^{-1} to a HTT of 900°C , the carbonized wood had 82 per cent of the bulk density of the precursor wood (Byrne and Nagle, 1997).

Mechanical strength

The mechanical strength of biochar is related to its solid density. Therefore, the increased molecular order of pyrolysed biomass gives it a higher mechanical strength than the biomass feedstock from which it was derived. For example, Byrne and Nagle (1997) reported that tulip poplar wood carbonized at a HTT of 1550°C had a 28 per cent increase in strength. Mechanical strength is a characteristic used for defining the quality of

activated carbon as it relates to its ability to withstand wear and tear during use. Agricultural wastes, such as nut shells (almond, hazelnut, macadamia and walnut) and fruit stones (apricot, olive pits, etc.) are of interest as activated carbons because of their high mechanical strength and hardness. These properties can be explained by high lignin and low ash contents (Aygun et al, 2003).

Future research

The physical properties of biochar products affect many of the functional roles that they may play in environmental management applications. The large variation of physical characteristics observed in different biochar products means that some will be more effective than others in certain applications. It is important that the physical characterization of biochars is undertaken before they are experimentally applied to environmental systems, and variations in outcomes may be correlated with these features. Although the

continued examination of the influence of feedstocks and processing conditions on the physical properties of biochars is essential, an important direction for future research is to develop an understanding of how and by what mechanisms these physical characteristics of biochars influence processes in soils. Further work is also required to determine how the physical properties of biochars change over time in soil systems and how these changes influence their function.

References

- Alaya, M. N., Girgis, B. S. and Mourad, W. E. (2000) 'Activated carbon from some agricultural wastes under action of one-step steam pyrolysis', *Journal of Porous Materials*, vol 7, pp509–517
- Amato, M. and Ladd, J. (1992) 'Decomposition of ^{14}C -labelled glucose and legume material in soils: Properties influencing the accumulation of organic residue and microbial biomass', *Soil Biology and Biochemistry*, vol 24, pp455–464
- Antal, M. J. and Grønli, M. (2003) 'The art, science, and technology of charcoal production', *Industrial Engineering and Chemical Research*, vol 42, pp1619–1640
- Aygun, A., Yenisoay-Karakas, S. and Duman, I. (2003) 'Production of granular activated carbon from fruit stones and nutshells and evaluation of their physical, chemical and adsorption properties', *Microporous and Mesoporous Materials*, vol 66, pp189–195
- Bansal, R. C., Donnet, J. B. and Stoeckli, F. (1988) *Active Carbon*, Marcel Dekker, New York, NY
- Biagini, E. and Tognotti, L. (2003) 'Characterization of biomass chars', in *Proceedings of the Seventh International Conference on Energy for Clean Environment*, 7–10 July 2003, Lisbon, Portugal
- Biscoe, J. and Warren, B. E. (1942) 'An X-ray study of carbon black', *Journal of Applied Physics*, vol 13, p364
- Boateng, A. A. (2007) 'Characterization and thermal conversion of charcoal derived from fluidized-bed fast pyrolysis oil production of switchgrass', *Industrial Engineering and Chemical Research*, vol 46, pp8857–8862
- Boehm, H. P. (1994) 'Some aspects of the surface chemistry of carbon blacks and other carbons', *Carbon*, vol 32, pp759–769
- Boehm, H. P. (2002) 'Surface oxides on carbon and their analysis: A critical assessment', *Carbon*, vol 40, pp145–149
- Bourke, J., Manley-Harris, M., Fushimi, C., Dowaki, K., Nunoura, T. and Antal, M. J. (2007) 'Do all carbonized charcoals have the same chemical structure? 2. A model of the chemical structure of carbonized charcoal', *Industrial Engineering and Chemical Research*, vol 46, pp5954–5967
- Brady, N. C. and Weil, R. R. (2008) *An Introduction to the Nature and Properties of Soils*, 14th edition, Prentice Hall, Upper Saddle River, NJ
- Braida W. J., Pignatello J. J., Lu, Y., Ravikovich P. I., Neimark A. V. and Xing B. (2003) 'Sorption hysteresis of benzene in charcoal particles', *Environmental Science and Technology*, vol 37, pp409–417
- Brown, R. A., Kercher, A. K., Nguyen, T. H., Nagle, D. C. and Ball, W. P. (2006) 'Production and characterization of synthetic wood chars for use as surrogates for natural sorbents', *Organic Geochemistry*, vol 37, pp321–333
- Byrne, C. (1996) *Polymer, Ceramic, and Carbon Composites Derived from Wood*, PhD thesis, The Johns Hopkins University, US
- Byrne, C. E. and Nagle, D. C. (1997) 'Carbonized wood monoliths – characterization', *Carbon*, vol 35, pp267–273
- Carmona, F. and Delhaes, P. (1978) 'Effect of density fluctuations on the physical properties of a disordered carbon', *Journal of Applied Physics*, vol 49, pp618–628
- Cetin, E., Moghtaderi, B., Gupta, R. and Wall, T. F. (2004) 'Influence of pyrolysis conditions on the structure and gasification reactivity of biomass chars', *Fuel*, vol 83, pp2139–2150
- Chan, K. Y., Van Zwieten, L., Meszaros, I., Downie, A. and Joseph, S. (2007) 'Agronomic values of greenwaste biochar as a soil amendment', *Australian Journal of Soil Research*, vol 45, pp629–634
- Emmerich, F. G. and Luengo, C. A. (1996) 'Babassu charcoal: A sulfurless renewable thermo-reducing feedstock for steelmaking', *Biomass and Bioenergy*, vol 10, pp41–44
- Emmerich, F. G., Sousa, J. C., Torriani, I. L. and Luengo C. A. (1987) 'Applications of a granular model and percolation theory to the electrical resistivity of heat treated endocarp of babassu nut', *Carbon*, vol 25, pp417–424
- Emmett, P. H. (1948) 'Adsorption and pore-size measurements on charcoal and whetlerites', *Chemical Reviews*, vol 43, pp69–148
- Franklin, R. E. (1951) 'Crystallite growth in graphitizing and non-graphitizing carbons', *Proceedings of the Royal Society of London, Series*

- A, Mathematical and Physical Sciences*, vol 209, pp196–218
- Freitas, J. C. C., Cunha, A. G. and Emmerich, F. G. (1997) 'Physical and chemical properties of a Brazilian peat char as a function of HTT', *Fuel*, vol 76, pp229–232
- Fukuyama, K., Kasahara, Y., Kasahara, N., Oya, A. and Nishikawa, K. (2001) 'Small-angle X-ray scattering study of the pore structure of carbon fibers prepared from a polymer blend of phenolic resin and polystyrene', *Carbon*, vol 39, pp287–290
- Gonzalez, M. T., Rodríguez-Reinoso, F., Garcia, A. N. and Marcilla, A. (1997) 'CO₂ activation of olive stones carbonized under different experimental conditions', *Carbon*, vol 35, pp159–162
- Gray, E., Marsh, H. and Robertson, J. (1985) 'Physical characteristics of charcoal for use in gunpowder', *Journal of Materials Science*, vol 20, pp597–611
- Guerrero, M., Ruiz, M. P., Millera, A., Alzueta, M. and Bilbao, R. (2008) 'Characterization of biomass chars formed under different devolatilization conditions: Differences between rice husk and eucalyptus', *Energy and Fuels*, vol 22, pp1275–1284
- Guo, J. and Lua, A. C. (1998) 'Characterization of chars pyrolyzed from oil palm stones for the preparation of activated carbons', *Journal of Analytical and Applied Pyrolysis*, vol 46, pp113–125
- Guo, J. and Rockstraw, D. A. (2006) 'Activated carbons prepared from rice hull by one-step phosphoric acid activation', *Microporous and Mesoporous Materials*, vol 100, pp12–19
- Hammes, K., Schmidt, M. W. I., Smernik, R. J., Currie, L. A., Ball, W. P., Nguyen, T. H., Louchouart, P., Houel, S., Gustafsson, Ö., Elmquist, M., Cornelissen, G., Skjemstad, J. O., Masiello, C. A., Song, J., Peng, P. A., Mitra, S., Dunn, J. C., Hatcher, P. G., Hockaday, W. C., Smith, D. M., Hartkopf-Froder, C., Bohmer, A., Luer, B., Huebert, B. J., Amelung, W., Brodowski, S., Huang, L., Zhang, W., Gschwend, P. M., Flores-Cervantes, D. X., Largeau, C., Rouzaud, J.-N., Rumpel, C., Guggenberger, G., Kaiser, K., Rodionov, A., Gonzalez-Vila, F. J., Gonzalez-Perez, J. A., de la Rosa, J. M., Manning, D. A. C., Lopez-Capel, E. and Ding, L. (2007) 'Comparison of quantification methods to measure fire-derived (black/elemental) carbon in soils and sediments using reference materials from soil, water, sediment and the atmosphere', *Global Biogeochemical Cycles*, vol 21, pGB3016
- Jankowska, H., Swiatkowski, A. and Choma, J. (1991) *Active Carbon*, Ellis Horwood, New York, NY
- Juma, N. (1993) 'Interrelationships between soil structure/texture, soil biota/soil organic matter and crop production', *Geoderma*, vol 57, pp3–30
- Kercher, A. K. and Nagle, D. C. (2002) 'Evaluation of carbonized medium-density fiberboard for electrical applications', *Carbon*, vol 40, pp1321–1330
- Kolb, S. (2007) *Understanding the Mechanisms by which a Manure-Based Charcoal Product Affects Microbial Biomass and Activity*, PhD thesis, University of Wisconsin, Green Bay, US
- Laine, J. and Yunes, S. (1992) 'Effect of the preparation method on the pore size distribution of activated carbon from coconut shell', *Carbon*, vol 30, pp601–604
- Laine, J., Simoni, S. and Calles, R. (1991) 'Preparation of activated carbon from coconut shell in a small scale concurrent flow rotary kiln', *Chemical Engineering Communications*, vol 99, pp15–23
- Lal, R. (2006) *Encyclopedia of Soil Science*, CRC Press, Boca Raton, FL
- Lewis, A. C. (2000) *Production and Characterization of Structural Active Carbon from Wood Precursors*, PhD thesis, Department of Materials Science and Engineering, The Johns Hopkins University, US
- Lima, I. M. and Marshall, W. E. (2005) 'Granular activated carbons from broiler manure: Physical, chemical and adsorptive properties', *Bioresource Technology*, vol 96, pp699–706
- Lua, A. C., Yang, T. and Guo, J. (2004) 'Effects of pyrolysis conditions on the properties of activated carbons prepared from pistachio-nut shells', *Journal of Analytical and Applied Pyrolysis*, vol 72, pp279–287
- Macias-García, A., Bernalte García, M. J., Díaz-Díez, M. A. and Hernandez Jimenez, A. (2004) 'Preparation of active carbons from a commercial holm-oak charcoal: Study of micro- and meso-porosity', *Wood Science and Technology*, vol 37, pp385–394
- Marsh, H. (1987) 'Adsorption methods to study microporosity in coals and carbons – a critique', *Carbon*, vol 25, pp49–58

- Marsh, H., Yan, D. S., O'Grady, T. M. and Wennerberg, A. (1984) 'Formation of active carbons from cokes using potassium hydroxide', *Carbon*, vol 32, pp603–611
- Martínez, M. L., Torres, M. M., Guzmán, C. A. and Maestri, D. M. (2006) 'Preparation and characteristics of activated carbon from olive stones and walnut shells', *Industrial Crops and Products*, vol 23, pp23–28
- Müller, T. and Höper, H. (2004) 'Soil organic matter turnover as a function of the soil clay content: Consequences for model applications', *Soil Biology and Biochemistry*, vol 36, pp877–888
- Oberlin, A. (2002) 'Pyrocarbons – review', *Carbon*, vol 40, pp7–24
- Pan, M. J. and van Staden, J. (1998) 'The use of charcoal in in vitro culture – a review', *Plant Growth Regulation*, vol 26, pp155–163
- Pandolfo, A. G., Amini-Amoli, M. and Killingley, J. S. (1994) 'Activated carbons prepared from shells of different coconut varieties', *Carbon*, vol 32, pp1015–1019
- Pastor-Villegas, J., Valenzuela-Calahorra, C., Bernalte-García, A. and Gómez-Serrano, V. (1993) 'Characterization study of char and activated carbon prepared from raw and extracted rockrose', *Carbon*, vol 31, pp1061–1069
- Pastor-Villegas, J., Pastor-Valle, J. F., Meneses Rodríguez, J. M. and García, M. (2006) 'Study of commercial wood charcoals for the preparation of carbon adsorbents', *Journal of Analytical and Applied Pyrolysis*, vol 76, pp103–108
- Pulido-Novicio, L., Hata, T., Kurimoto, Y., Doi, S., Ishihara, S. and Imamura, Y. (2001) 'Adsorption capacities and related characteristics of wood charcoals carbonized using a one-step or two-step process', *Journal of Wood Science*, vol 47, pp48–57
- Puziy, A. M., Poddubnaya, O. I., Martínez-Alonso, A., Suárez-García, F. and Tascon, J. M. D. (2005) 'Surface chemistry of phosphorus-containing carbons of lignocellulosic origin', *Carbon*, vol 43, pp2857–2868
- Qadeer, R., Hanif, J., Saleem, M. A. and Afzal, M. (1994) 'Characterization of activated charcoal', *Journal of the Chemical Society of Pakistan*, vol 16, pp229–235
- Rodríguez-Mirasol, J., Cordero, T. and Rodríguez, J. J. (1993) 'Preparation and characterization of activated carbons from eucalyptus kraft lignin', *Carbon*, vol 31, pp87–95
- Rodríguez-Reinoso, F. (1997) *Introduction to Carbon Technologies*, Universidad de Alicante, Alicante, Spain
- Rodríguez-Reinoso, F. and Molina-Sabio, M. (1992) 'Activated carbons from lignocellulosic materials by chemical and/or physical activation: An overview', *Carbon*, vol 30, pp1111–1118
- Rouquerol, F., Rouquerol, I. and Sing, K. (1999) *Adsorption by Powders and Porous Solids*, Academic Press, London, UK
- Setton, R., Bernier, P. and Lefrant, S. (2002) *Carbon Molecules and Materials*, CRC Press, Boca Raton, FL
- Shamsuddin, A. H. and Williams, P. T. (1992) 'Devolatilisation studies of oil-palm solid wastes by thermo-gravimetric analysis', *Journal of the Institute of Energy*, vol 65, pp31–34
- Sjöström, E. (1993) *Wood Chemistry: Fundamentals and Applications*, second edition, Academic Press, San Diego, US
- Stavropoulos, G. G. (2005) 'Precursor materials suitability for super activated carbons production', *Fuel Processing Technology*, vol 86, pp1165–1173
- Troch, F. R. and Thompson, L. M. (2005) *Soils and Soil Fertility*, Blackwell Publishing, Iowa, US
- Wang, S.-Y., Tsai, M.-H., Lo, S.-F., Tsai, M.-J. (2008) 'Effects of manufacturing conditions on the adsorption capacity of heavy metal ions by Makino bamboo charcoal', *Bioresource Technology*
- Warren, B. E. (1941) 'X-ray diffraction in random layer lattices', *Physical Review*, vol 59, pp693–698
- Wildman, J. and Derbyshire, F. (1991) 'Origins and functions of macroporosity in activated carbons from coal and wood precursors', *Fuel*, vol 70, pp655–661
- Zabaniotou, A., Stavropoulos, G. and Skoulou, V. (2008) 'Activated carbon from olive kernels in a two-stage process: Industrial improvement', *Bioresource Technology*, vol 99, pp320–326
- Zhang, T., Walawender, W. P., Fan, L. T., Fan, M., Dugaard, D. and Brown, R. C. (2004) 'Preparation of activated carbon from forest and agricultural residues through CO₂ activation', *Chemical Engineering Journal*, vol 105, pp53–59